Vibrational Spectrum of Cd^{112}†*

P. D. BARNES,‡ J. R. COMFORT, AND C. K. BOCKELMAN
Nuclear Structure Laboratory, Yale University, New Haven, Connecticut
(Received 14 November 1966)

The energies and angular distributions of proton groups produced in the $Cd^{111}(d,p)Cd^{112}$ reaction were measured with an over-all resoltuion of 20 keV. A distorted-wave analysis, employing experimentally determined optical-model parameters, was used to extract values of l_n and spectroscopic strengths for states up to 3.3-MeV excitation in Cd^{112}. Wave functions of Cd^{111} and Cd^{112} calculated in the random-phase approximation are tested both by comparison of sum-rule predictions with the summed spectroscopic factors, and by comparison of individual spectroscopic factors with those predicted by the microscopic theory of nuclear vibrations for states in Cd^{111} and the zero-, one-, and two-phonon states in Cd^{112}.

I. INTRODUCTION

THE low-lying energy levels of spherical medium-weight even-even nuclei may be described in terms of collective vibrations of the nuclear surface.[1] Such analysis in terms of harmonic quadrupole vibrations is suggested by the approximately equal level spacings observed between the 0_1^+, 2_1^+, and 2_2^+ levels, the enhanced nature of the reduced transition rates $B(E2, 0_1^+ \rightarrow 2_1^+)$ and $B(E2, 2_1^+ \rightarrow 2_2^+)$, the comparatively retarded transition rates $B(E2, 0_1^+ \rightarrow 2_2^+)$, and, in some cases, the observation of the approximately degenerate triplet of the states 0_2^+, 2_2^+, and 4_1^+ at twice the excitation energy of the 2_1^+ level.

In recent years a microscopic description of harmonic vibrations has been formulated in terms of residual interactions between shell-model particles. At low excitation energies the important parts of the residual two-nucleon interaction are represented by a pairing and a long-range force.[2] Many authors have discussed approximation methods for solving the resulting many-body Hamiltonian.[3–9] The technique of linearized equations (also called the random-phase approximation method and abbreviated hereafter as RPA) has been systematically applied to medium-weight nuclei by Kisslinger and Sorenson.[9]

With regard to the experimental properties listed above, the even Cd isotopes would appear to be good harmonic vibrators.[10] The relevant data for Cd^{112} are presented in Fig. 1. However, the recent measurements of DeBoer *et al.*[11] and Stelson *et al.*[12] indicate that the 2_1^+ state of Cd^{114} is also characterized by a large static quadrupole moment, i.e., -0.7 b, compared with -0.077 b predicted by the RPA.[13] In order to explore the microscopic implications of this problem, it is interesting to test the detailed structure of the RPA wave functions for these collective, but apparently

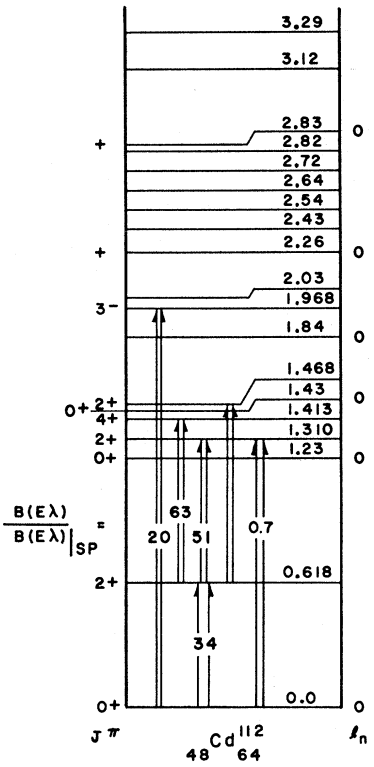

FIG. 1. The level scheme of Cd^{112}. This diagram is based on the data summarized in the *Nuclear Data Sheets* (Ref. 20). The arrows indicate the transitions observed in the Coulomb excitation work of McGowan *et al.* (Ref. 10); the transition rates measured in single-particle units are indicated, as are the l_n values from the (d,p) experiments of Ref. 19.

† Supported in part under Contract No. AT(30-1)3223 with the U. S. Atomic Energy Commission.
* Portions of this work were submitted by P. D. Barnes to Yale University in partial fulfillment of the requirements for the Ph.D. Degree.
‡ Present address: Los Alamos Scientific Laboratory, Los Alamos, New Mexico.
[1] G. Scharff-Goldhaber and J. Weneser, Phys. Rev. **98**, 212 (1955).
[2] S. T. Belyaev, Kgl. Danske Videnskab. Selskab, Mat. Fys. Medd. **31**, No. 11 (1959).
[3] M. Baranger, Phys. Rev. **120**, 957 (1960).
[4] D. J. Thouless, Nucl. Phys. **22**, 78 (1961).
[5] T. Marumori, Progr. Theoret. Phys. (Kyoto) **24**, 331 (1960).
[6] T. Tamura and T. Udagawa, Progr. Theoret. Phys. (Kyoto) **26**, 947 (1961).
[7] R. Arvieu and M. Veneroni, Compt. Rend. **250**, 992 (1960); **250**, 2155 (1960).
[8] S. Yoshida, Nucl. Phys. **38**, 380 (1962).
[9] L. S. Kisslinger and R. A. Sorenson, Rev. Mod. Phys. **35**, 853 (1963).
[10] F. K. McGowan, R. L. Robinson, P. H. Stelson, and J. L. C. Ford, Jr., Nucl. Phys. **66**, 97 (1965).
[11] J. DeBoer, R. G. Stokstad, J. P. Symons, and A. Winther, Phys. Rev. Letters **14**, 564 (1965); R. G. Stokstad, I. Hall, G. D. Symons, and J. DeBoer, Nucl. Phys. **A92**, 319 (1967).
[12] P. H. Stelson, W. T. Milner, J. L. C. Ford, Jr., F. K. McGowan, and R. L. Robinson, Bull. Am. Phys. Soc. **10**, 427 (1965).
[13] T. Tamura and T. Udagawa, Phys. Rev. Letters **15**, 765 (1965).

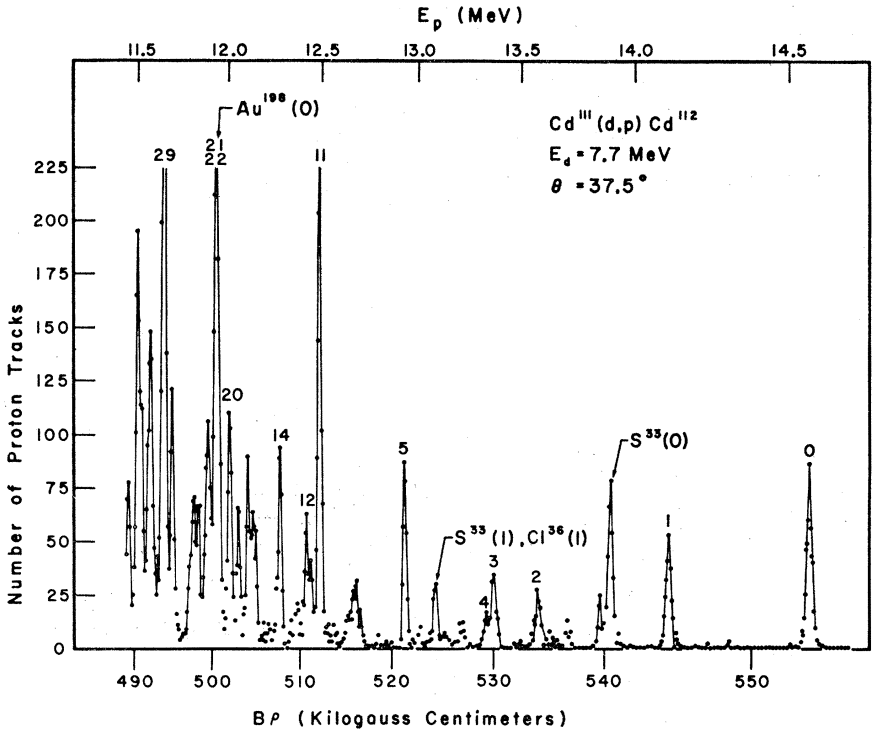

FIG. 2. Proton spectrum observed at laboratory angle 37.5°. The number of proton tracks in a 0.5-mm strip across the exposed zone is graphed as a function of proton momentum (kG cm) and energy (MeV). Peaks corresponding to levels in Cd^{112} are numbered as in Table III. Prominent peaks associated with contaminants in the target are also identified.

anharmonic states. The present work is concerned with such a test; it reports measurements of the spectroscopic factors for the excitation of these states in the $Cd^{111}(d,p)Cd^{112}$ reaction. A companion paper[14] discussing a $Cd^{113}(d,p)Cd^{114}$ experiment performed under similar experimental conditions is in preparation. In these reports, the experimental values are compared with the predictions of the RPA wave functions for zero-, one-, and two-phonon final states. Experimental results for higher excited states in Cd^{112} and Cd^{114} are also presented.

II. EXPERIMENTAL PROCEDURE

The data reported here were obtained in three separate runs, each using a different Cd target.

The proton angular distributions were obtained using a target produced by vacuum evaporation of Cd metal enriched in Cd^{111} onto a 100-$\mu g/cm^2$ self-supporting gold foil. The isotopic composition of the 20-$\mu g/cm^2$ layer of Cd metal is indicated in Table I. The main impurities observed in the spectra were $C^{12,13}$, N^{14}, O^{16}, Si^{28}, S^{32} and trace amounts of Cl^{35}, Cu^{63}, and Cu^{65}. This target was exposed to 7.7-MeV deuterons from the MIT-ONR Van de Graaff accelerator. The reaction products were momentum analyzed in the MIT 24-gap spectrograph[15] and detected with 50-μ NTA nuclear emulsions. Tantalum and aluminum foils covered the emulsions to prevent all particles except protons from being recorded. Approximately 13 000 μC passed through the target in a 15-h exposure.

The developed emulsions were scanned for proton tracks in 0.5-mm strips, i.e., 5-keV-wide channels. A typical spectrum is shown in Fig. 2, where the observed track density is graphed as a function of proton energy. Proton groups corresponding to states in cadmium as well as those resulting from contaminants are indicated. The observed linewidth is about 20 keV.

As a result of differential hysteresis in the 24-gap spectrograph, a Q-value scale could only be established by using effective magnetic fields for each gap. The magnitudes of these fields were obtained by demanding that 48 easily recognized impurity groups have Q values consistent with those given in the literature. The

TABLE I. The isotopic composition of the Cd^{111} target. The enriched material was obtained from the Isotope Sales Division of the Oak Ridge National Laboratory. Column (1) lists the various stable isotopes of natural cadmium. Column (2) gives the relative abundances of these isotopes in the Cd^{111} target as obtained in a spectroscopic analysis performed at Oak Ridge.

Cadmium isotope	Percent abundance
106	0.11
108	0.06
110	1.65
111	89.9
112	6.2
113	0.82
114	1.16
116	0.21

[14] J. R. Comfort, C. K. Bockelman, and P. D. Barnes, Phys. Rev. (to be published).
[15] H. Enge and W. W. Buechner, Rev. Sci. Instr. 34, 155 (1963).

relation between distance along the plate and "radius of curvature" is based on an energy standard of 5.3042±0.0016 MeV for Po^{210} α particles.

The effective fields were used for identification of the mass associated with each particle group by observation of the change of particle energy with angle. It was possible to identify all peaks associated with proton momentum greater than that corresponding to 3.5 MeV of excitation in cadmium. For groups associated with lower momenta the increasing density of peaks from reactions in both cadmium and gold, combined with the decreasing dispersion of the spectrometer, made analysis unreliable. The effective fields also furnished a Q-value scale for the cadmium levels which was self-consistent to within ±5 keV. The level excitations are considered known to ±8 keV. The Q value for the Cd^{112} ground-state transition was measured as 7.171±0.010 MeV.

Use of this target for measurement of the scattering cross sections was precluded by the gold backing, which produced an elastically scattered deuteron group not easily separated from the Cd group. Therefore, a target of Cd in natural abundance was prepared by vacuum evaporation onto a thin Formvar backing. Such targets were difficult to prepare; Cd does not adhere to this backing readily. However, one such target was used in a separate series of spectrograph exposures to measure the angular distribution of 7.7-MeV deuterons elastically scattered by natural cadmium. The distribution, which was used to provide information on the optical-model parameters to be applied in the distorted-wave Born-approximation (DWBA) calculations, is shown in Fig. 3. The cross-section scale was obtained by comparison with the yield from the same target with 2.5-MeV deuterons incident. It is assumed that the elastic deuteron scattering from Cd follows the Rutherford law at 2.5 MeV. (The Coulomb barrier in Cd is 9 MeV.) The normalization error on the 7.7-MeV elastic-scattering cross section is estimated to be ±7% in addition to the statistical error shown for individual data points.

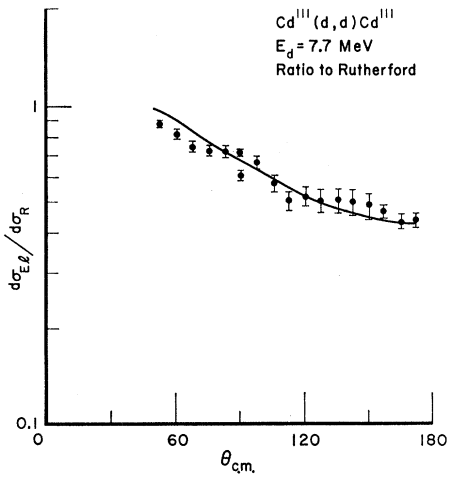

FIG. 3. The differential cross section for elastic scattering of 7.7 MeV deuterons on natural cadmium expressed in ratio to the calculated Rutherford cross section. The numbers are based on the assumption that the elastic scattering of 2.5 MeV deuterons on cadmium follows the Rutherford law. The vertical bars indicate statistical errors only. The solid line represents the cross section calculated from the deuteron optical potential using the parameters listed in Table II

In order to provide an absolute-cross-section scale for the (d,p) reaction, an additional measurement of the ratio of (d,p) to (d,d) yields was made on the single-gap broad-range spectrograph at Argonne National Laboratory. A third target was used. It consisted of a Formvar backing onto which was evaporated a very thin layer of gold, followed by a layer of natural cadmium. The Au layer was thin enough to permit good separation of the elastically scattered Au and Cd groups, yet was sufficiently thick that the Cd layer adhered to it nicely.[16] A 16 000-μC exposure of this target to 7.7-MeV deuterons established the yield for (d,p) reactions going to the ground state and three excited states of Cd^{112}. Both before and after this (d,p) exposure, the 7.7-MeV elastic deuteron yield of the target was measured. The resultant peaks indicated a 20% increase in target thickness during the period of the (d,p) exposure. The apparent increase suggests that the targets were not uniform in thickness and that the distribution of beam intensity over the illuminated area of the targets changed significantly during the run. Compounding the uncertainty in target thickness with the error in the elastic-scattering cross section and a 6% statistical error leads to an estimated error in the absolute (d,p) cross-section scale of ±20%.

III. ANALYSIS AND RESULTS

A. Distorted-Wave Analysis

The differential cross section representing the observed proton angular distributions is given as

$$\frac{d\sigma}{d\Omega}=\frac{3}{2}\frac{2J_f+1}{2J_i+1}\sum_{l,j}S_{lj}\sigma_l(\theta), \qquad (1)$$

where J_i and J_f are the total angular momenta of the target and residual nuclei and the factor $\frac{3}{2}$ is associated with the use of a Hulthén wave function for the deuteron. The spectroscopic factor S_{lj} is discussed in Sec. IV. The factor $\sigma_l(\theta)$ is a theoretical estimate of the probability that there will be a transition from the incident deuteron channel to an outgoing proton channel with the neutron captured into a single-particle orbit labeled by the orbital and total angular momenta l and j, respectively. In this experiment all calculations have been done in the distorted-wave approximation through the use of the computer code JULIE written by Drisko.[17] The calculations are zero range and use local

[16] We are grateful to R. Smithers and J. Erskine for suggesting this technique to us.

[17] R. H. Bassel, R. M. Drisko, and G. R. Satchler, Oak Ridge National Laboratory Report No. 3240, 1960 (unpublished).

TABLE II. Parameters used in the distorted-wave calculations. The real well depths V and imaginary well depths W' are given in MeV, and the lengths in F. The real well depth of the proton optical potential was varied according to the relation $V=V_0-0.32E_p$, where E_p is the proton energy and $V_0=60.1$ MeV.

Particle	V	W'	r_0	a	r_0'	a'	r_c
n			1.25	0.65			1.25
p	$\geqslant 55.3$	9.6	1.20	0.68	1.21	0.73	1.25
d	85.0	19.9	1.24	0.78	1.316	0.68	1.24

potentials. A Woods-Saxon potential is used to bind the transferred neutron to the target core, the well depth being adjusted to yield the observed neutron binding energy for each state. Wave functions for the deuteron and proton channels were determined from optical potentials containing real Woods-Saxon, imaginary surface-derivative, and Coulomb terms. Considerable care was exercised in choosing the parameters of the proton and especially the deuteron optical potentials; the details of these considerations will be described in the subsequent publication on the $Cd^{113}(d,p)Cd^{114}$ reaction.[14] The same parameters have been used in the calculations for both reactions and are listed in Table II.

B. Results

Some typical proton angular distributions are shown in Figs. 4–13. The dots are experimental points with the bars indicating statistical uncertainties. The solid lines are the DW calculations. A comparison of the predicted proton angular distributions indicated that the neutron orbits $l_n=0$–4 could be distinguished. The $l_n=5$ case was neither calculated nor identified. The $\frac{1}{2}^+$ character of the target and conservation of angular momentum and parity require that only one l_n can contribute to the excitation of a final state of natural parity, i.e., $\pi=(-1)^J$.

Table III lists all the states observed in Cd^{112}. The

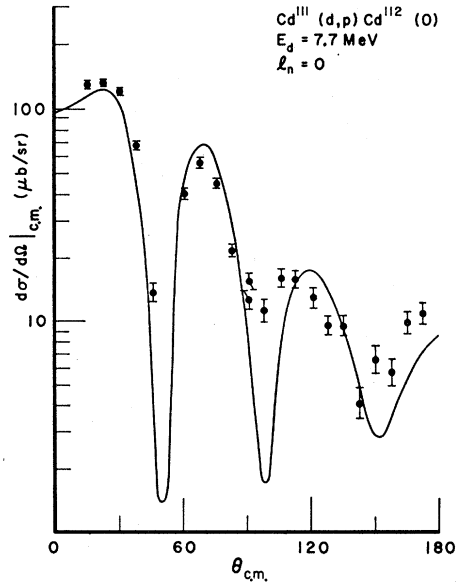

FIG. 4. The absolute differential cross section for the formation of the ground state of Cd^{112}. The error bars indicate statistical errors only, and do not include the 20% error in absolute cross section. In subsequent figures, vertical arrows indicate cases in which contributions from contaminants may be present in unknown amounts, so that only an upper limit to the intensity can be established. The solid line is the distorted-wave fit using the parameters listed in Table II. The excitation energy and transition strength are listed in Table III.

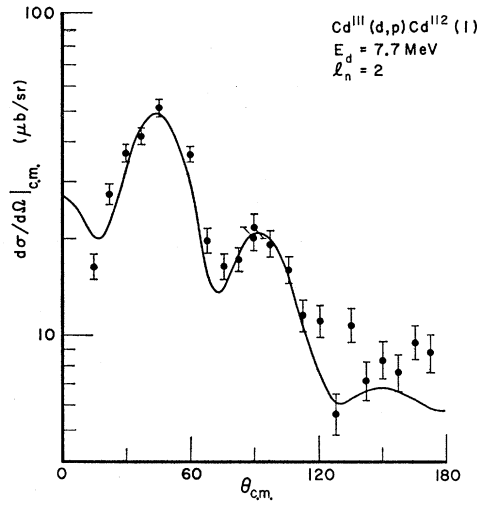

FIG. 5. The absolute differential cross section for the formation of the first excited state of Cd^{112}, here interpreted as a quadrupole one-phonon state. See also the caption of Fig. 4.

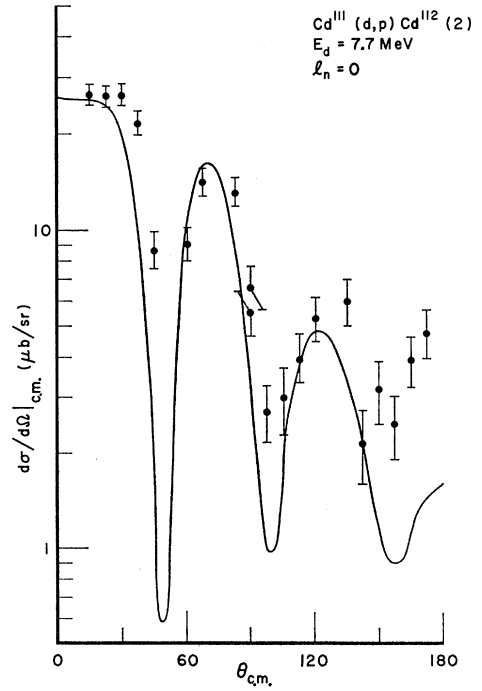

FIG. 6. The absolute differential cross section for the formation of state (2) of Cd^{112}, here interpreted as the 0^+ component of the two-phonon state. See also the caption of Fig. 4.

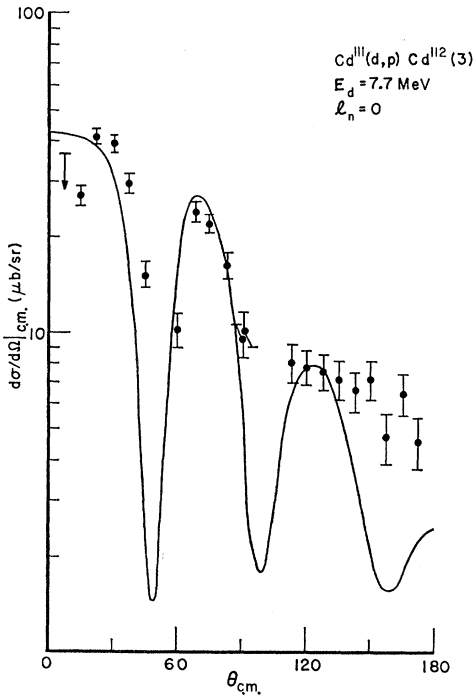

FIG. 7. The absolute differential cross section for the formation of state (3) of Cd^{112}. See also the caption of Fig. 4.

ground-state Q value was measured as 7.171 ± 0.010 MeV and the level excitations (column 2) are known to ±8 keV (see Sec. II). Wherever possible the angular

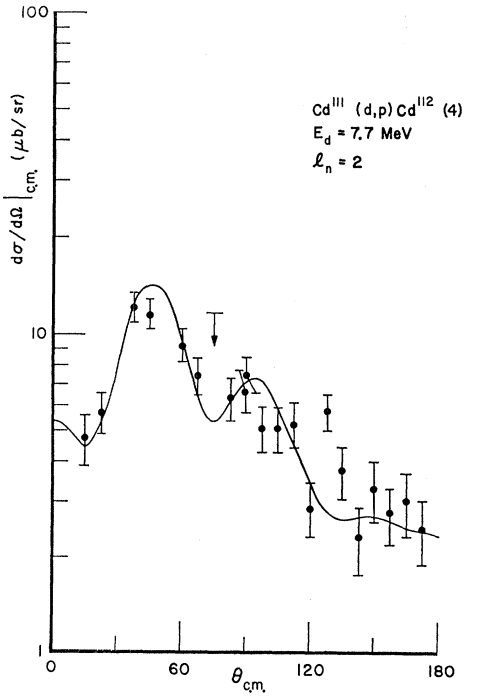

FIG. 8. The absolute differential cross section for the formation of state (4) of Cd^{112}. See also the caption of Fig. 4.

TABLE III. Levels observed in Cd^{112}. Column 1 is a code number identifying each observed level. Column 2 gives the excitation energies in Cd^{112} based on a ground-state Q value of 7.171 MeV. Columns 3, 4, and 5 give the value of l_n, π, and the transition strength $(2J_f+1)S_{lj}$ suggested by the analysis of the observed differential cross section within the framework of the distorted-wave approximation. Column 7 is the value of S_{lj} obtained from column 5 by using the final-state spins listed in column 6. Column 8 lists the maximum observed differential cross section.

No.	E_x (MeV)	l_n	π	$(2J+1)S_{lj}$	J_f	S_{lj}	$d\sigma/d\Omega\|_{max}$ (μb/sr)
0	0.000	0	+	0.28	0	0.28	133.0
1	0.619	2	+	0.36	2	0.072	51.3
2	1.228	0	+	0.051	0	0.051	26.4
3	1.436	0	+	0.078	0	0.078	41.5
4	1.474	2	+	0.095	2	0.019	12.1
5	1.876	0	+	0.11			$\leq$72.1
6	2.009	(2,3)		(0.033,0.060)			5.0
7	2.087	...		...			4.8
8	2.123	2	+	0.13			$\leq$23.6
9	2.159	2	+	0.089			14.6
10	2.235	(2,3)		(0.042,0.067)			6.2
11	2.302	0	+	0.22			164.0
12	2.374	...		...			42.4
13	2.424	(0,1)		...			21.6
14	2.507	2	+	0.38			$\leq$67.4
15	2.573	...		...			$\leq$10.4
16	2.637	2	+	0.24			48.5
17	2.657	...		...			$\leq$47.0
18	2.678	2	+	0.35			62.9
19	2.725	2	+	0.32			$\leq$64.1
20	2.770	2	+	0.39			$\leq$88.3
21	2.822						
22	2.840	(0+2)		...			$\leq$204.5
23	2.875	...		...			$\leq$89.0
24	2.901	...		...			$\leq$89.0
25	2.936	2	+	0.27			62.0
26	2.965	2	+	0.30			$\leq$75.8
27	2.988	...		...			$\leq$75.8
28	3.071	...		...			$\leq$83.1
29	3.113	2	+	1.45			$\leq$284.0
30	3.184	2	+	0.83			161.0
31	3.240	...		...			155.0
32	3.304	2	+	0.32			76.0
33	3.344	...		...			$\leq$77.2

distributions were fitted by DW curves for a single l_n, listed in column 3. However, the presence of an $l_n=2$ component in an $l_n=0$ state is difficult to detect, and the data at small angles for some states assigned $l_n=2$ do not preclude the admixture of an $l_n=0$ component (e.g., Fig. 13). For state (11), $l_n=0$ appears to be the only possible fit, but as shown in Fig. 10, the experimental cross section at small angles shows a dip not predicted by the DW calculation. Copies of the complete set of angular distributions may be obtained from the authors.

The quantity $(2J_f+1)S_{lj}$ (hereafter called the strength of the transition), the total angular momentum of the final state, J_f (where known from the literature), and the spectroscopic factor S_{lj} derived from the distorted-wave calculations are listed in columns 5–7 of Table III. The maximum differential cross section observed for each group is given in column 8. It is extremely difficult to assess the error which should be assigned to the transition strengths. The uncertainty in

absolute cross section implies a 20% error. Trial distorted-wave calculations indicate that the latitude of the uncertainties in the proton and deuteron optical-model parameters permitted by the measured angular distributions imply a 30% uncertainty in the strengths. Even larger uncertainties may be incurred by the use of an approximate neutron wave function in code JULIE and by the neglect of effects of target excitation, finite range, etc. While the total effect of such uncertainties cannot be quantitatively calculated, drawing on general experience in this type of calculation, an over-all error of a factor of 2 in the transition strengths appears reasonable.

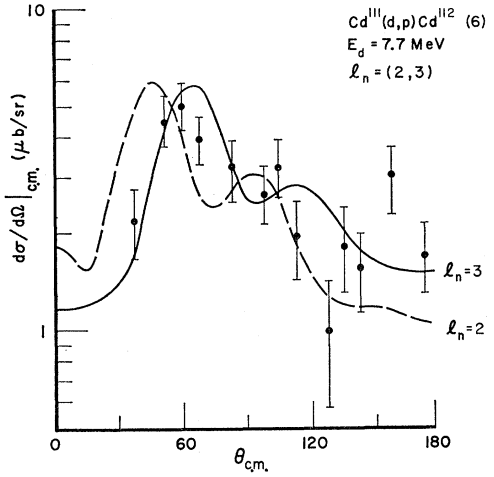

FIG. 9. The absolute differential cross section for the formation of state (6) of Cd^{112}. See also the caption of Fig. 4. The angular distribution indicates that a deuteron stripping component is present but the poor statistical accuracy precludes a definite choice of l_n.

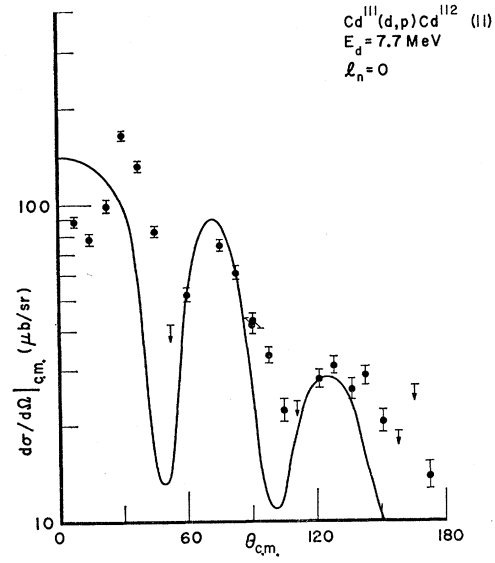

FIG. 10. The absolute differential cross section for the formation of state (11) of Cd^{112}. See also the caption of Fig. 4. This angular distribution cannot be fit by $l_n>0$, yet the dip at forward angles does not follow the distorted-wave prediction.

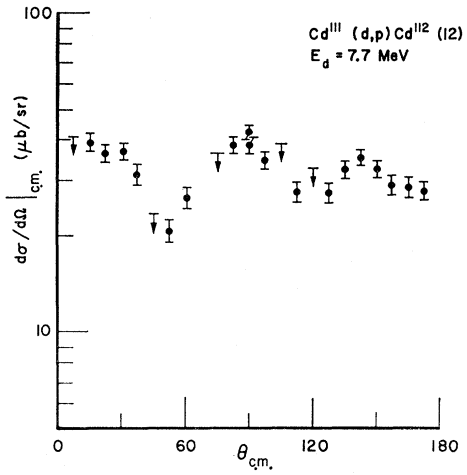

FIG. 11. The absolute differential cross section for the formation of state (12) in Cd^{112}. See also the caption for Fig. 4. The angular distribution does not fit a distorted-wave prediction for any single $l_n<5$.

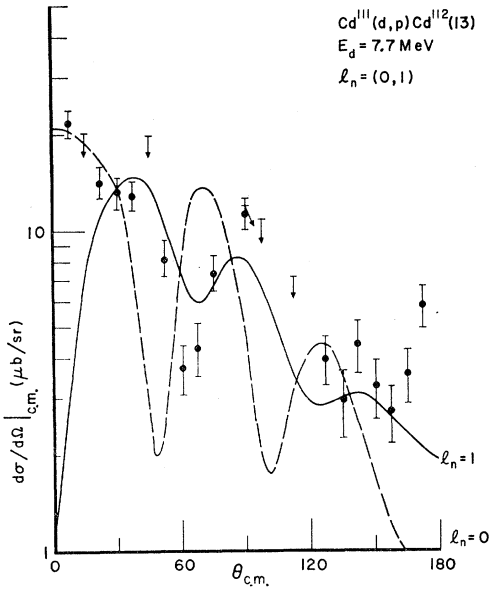

FIG. 12. The absolute differential cross section for the formation of state (13) of Cd^{112}. See also the caption for Fig. 4. The angular distribution indicates that a deuteron stripping component is present, and the shape indicates a mixture of $l_n=0$ and 1, implying that more than one state is present.

Recent data relevant to the level scheme of Cd^{112} are summarized in the work of Girgis and van Lieshout,[18] who studied β decay of Ag^{112}, in the (d,p) experiment of Cohen and Price[19] at 14.9-MeV deuteron energy, and in the Coulomb-excitation work of McGowan *et al.*[10] These results are shown in Fig. 1, which lists the level diagram

[18] R. Girgis and R. Van Lieshout, Physica **25**, 1200 (1959).
[19] B. Cohen and R. Price, Phys. Rev. **118**, 1582 (1960).

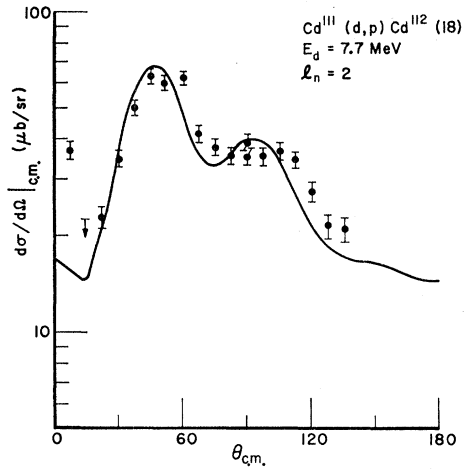

FIG. 13. The absolute differential cross section for the formation of state (18) of Cd^{112}. See also the caption for Fig. 4. The high point at $\theta_{c.m.}=7.6°$ may signify a small $l_n=0$ component.

as given in the *Nuclear Data Sheets*,[20] with additions from Ref. 10. The present measurements listed in Table III are in good agreement with the previous work for excitations below 2 MeV. Two members of the "phonon triplet," the 2_2^+ level at 1.310 MeV and the 4_1^+ level at 1.413 MeV, are not observed in the present work. Upper limits for the maximum differential cross section for these states are estimated as 10 μb/sr and 4 μb/sr, respectively. [The 2_2^+ level was observed in the earlier (d,p) experiment.[19]]

Above 2-MeV excitation the present experiment reveals a greater level density than is shown on Fig. 1. However, this is not unexpected in view of the greater selectivity of the β-decay process and, in comparison to the earlier (d,p) work, the improved resolution (20 keV as compared to 75 keV). For the stronger levels above 2 MeV, the agreement with Cohen and Price[19] is good.

The angular correlation data of Simons *et al.*[21] yield spins for several levels not identified in Fig. 1. Their measurement of $J=2$ or 4 for a 2.250-MeV state suggests that it be identified with state (10) in Table III, while the 2.28-MeV level of Cohen and Price[19] is state (11). The $J=2$ level at 2.440 MeV[21] appears to be level (13), for which the present angular distribution data does not clearly define a l_n. The $J=1$ or 3 level at 2.740 MeV[21] may be identified with our level (19). Unfortunately, the forward angles for level 19 were obscured, so that an $l_n=0$ contribution cannot be excluded; no choice between the two values of J is determined by the present data.

[20] *Nuclear Data Sheets*, compiled by K. Way *et al.* (Printing and Publishing Offices, National Academy of Sciences—National Research Council, Washington 25, D. C., revised 1964).

[21] L. Simons, K. E. Nystén, H. Junger, P. Holmberg, and F. Stenman, Soc. Sci. Fennica, Commentationes Phys.-Math. **28**, No. 3 (1963).

IV. DISCUSSION

The spectroscopic factor S_{lj} appearing in Eq. (1) is defined as

$$S_{lj}=\left[\int \Psi_{J_fM_f}[\Phi_{jm}\Psi_{J_iM_i}]_{J_fM_f}d\tau\right]^2. \quad (2)$$

Here Φ_{jm} describes the captured neutron in the orbit $(nljm)$, and $\Psi_{J_iM_i}$ and $\Psi_{J_fM_f}$ are the wave functions of the initial and final system with total angular momenta J_i, J_f and z components M_i and M_f, respectively.

The absolute magnitudes of the above overlap integrals for states in Cd^{112} implied by the present experimental measurements are listed in Table III, column 7. We have also calculated these quantities using the microscopic wave functions proposed by Baranger[3] for the description of harmonic nuclear vibrations. These wave functions have been discussed by many authors. We have used the formalism of Yoshida,[8] extending his calculations to the particular cases of interest here.

In a shell-model description of an even-even nucleus in which the residual interaction is approximated by a pairing force, the ground state (quasiparticle vacuum) is separated from the lowest two-quasiparticle states by an energy gap 2Δ. When a long-range force is also included in the residual interaction, collective states are lowered into the energy gap. If the quadrupole-quadrupole long-range interaction is used and treated by the method of linearized equations, then the collective state has the properties of a harmonic quadrupole vibration. A two-phonon triplet of vibrational states ($J^\pi=0^+$, 2^+, 4^+) is predicted at twice this excitation energy. Above the energy gap, a sharp increase in the number of states is expected.

The expected distribution of states is observed qualitatively in the spectrum of Cd^{112} as illustrated in the strength function shown in Fig. 14. The states below an energy of 2.5 MeV corresponding to the neutron energy gap are rather weakly excited. Above this energy the strength increases by more than a factor of five for states that are basically two quasiparticle in character. The calculated positions of pure two-quasiparticle states in the absence of a long-range force are indicated. The ground and first excited states are interpreted as no-phonon and one-phonon states. Of the known 0_2^+, 2_2^+, 4_1^+ triplet, here interpreted as the two-quadrupole phonon states, only the 0_2^+ second excited state at 1.23 MeV is observed in the present experiment. With regard to the approximations to be used below, it is important to note that the triplet appears at half the energy of the neutron energy gap $2\Delta_n$.

In general the properties of a system of shell-model particles interacting with both a pairing and a λ-pole force are expressible in terms of the following parameters: ϵ_j, the shell-model energy of the orbit (nlj); G, the strength of the pairing interaction (effective be-

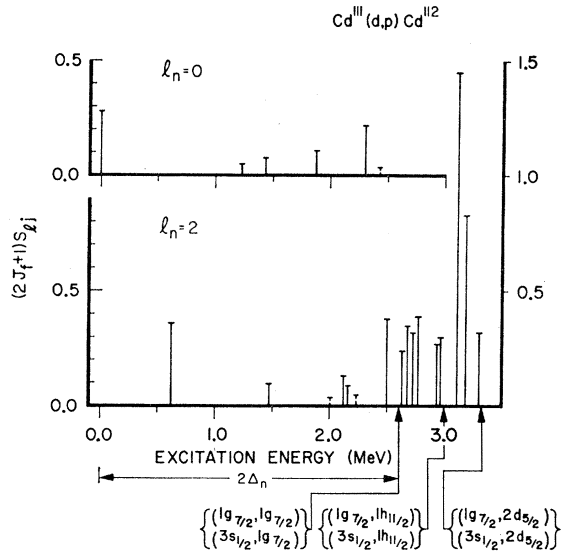

FIG. 14. The observed strength function $(2J_f+1)Sl_j$ for Cd^{112}. This is a graph of columns (2) and (5) of Table III. The magnitude of $2\Delta_n$ and the positions of the lowest two-quasiparticle neutron levels using the parameters of Table IV are indicated.

tween like nucleons); and χ_λ, the interaction strength of the λ-pole force (effective between any pair of nucleons). The Hamiltonian of such a system [Eq. (2.1) in Ref. 8] has not been diagonalized in the case of medium-weight nuclei. However, in order to obtain approximate wave functions for the low-lying states in both even and odd nuclei, one can introduce the Bogoliubov-Valatin transformation in order to treat the pairing force, and solve the transformed Hamiltonian eigenequation by the method of linearized equations. In this approximation, one looks for a solution $\Psi_{\lambda\mu}$ for the even system such that if Φ is an energy eigenfunction with eigenvalue E, then

$$\Psi_{\lambda\mu}=Q_{\lambda\mu}^{\dagger}\Phi$$
$$=\tfrac{1}{2}\sum_{j_1j_2}[R_{j_1j_2}^{\lambda}A^{\dagger}(j_1j_2\lambda\mu)-T_{j_1j_2}^{\lambda}(-1)^{\lambda-\mu}A(j_1j_2\lambda-\mu)]\Phi \quad (3)$$

is also an eigenfunction with energy eigenvalue $E'=E+\hbar\omega$.

$Q_{\lambda\mu}^{\dagger}$ can be interpreted as a phonon-creation operator (especially the lowest-energy solution of this form). The ground state Ψ_0 with energy E_0 has no phonons and is determined by the condition $Q_{\lambda\mu}\Psi_0=0$. The operator $A^{\dagger}$ (A) is composed of angular-momentum-coupled pairs of quasiparticle creation (annihilation) operators [Eq. (2.13) of Ref. 8]. In the random-phase approximation, the amplitudes $R_{j_1j_2}^{\lambda}$ and $T_{j_1j_2}^{\lambda}$ can be expressed in closed form [Eq. (2.34) of Ref. 8].

Finally, for an even-even nucleus the general wave function for which N phonons are coupled to JM is expressed as

$$\Psi_{NJM}=[Q_{\lambda\mu_1}^{\dagger}Q_{\lambda\mu_2}^{\dagger}\cdots Q_{\lambda\mu_N}^{\dagger}]_{J,M,v}\Psi_0\equiv|Nv,JM\rangle, \quad (4)$$

where v represents any additional quantum numbers necessary to describe the coupling.

In an odd-A system, the λ-pole force introduces a coupling between the degrees of freedom of the core (phonon states) and the excitations of the odd quasiparticle. Therefore, the wave functions are expressed as a superposition of the form

$$\Psi_{JM}=\sum_{j,N,v,I}C_{jNvIJ}|j,NvI,JM\rangle, \quad (5)$$

where the base function $|j, NvI, JM\rangle$ of total angular momentum J, M is formed from coupling a quasiparticle in the orbit j to a system of N phonons coupled to a spin I. With up to two phonons included in the sum, Eq. (5), the coefficients C_{jNvIJ} are determined in the present work by a complete diagonalization of the Hamiltonian for the odd-particle system [Eq. (3.8), Ref. 8] for a $\lambda=2$ interaction.

The problem of testing the approximations of this model through a comparison of spectroscopic factors becomes one of (a) making a suitable choice of the model parameters identified above; (b) calculating and comparing the description of the odd A (target) nucleus with experimentally determined quantities in order to test the applicability of the calculated ground-state wave function $\Psi_{J_iM_i}$; (c) evaluating the spectroscopic factor S_{lj} for transitions from the ground state of the odd system to states of zero-, one-, and two-phonon excitations in the even system.

A. Choice of Parameters

The RPA calculations being treated here are completely specified by the proton and neutron quasiparticle energies E_j and the coupling parameter for the quadrupole force χ_2. Neither the presence of higher multipole interactions nor the possibility that χ may be different for n-n, p-p, and n-p interactions is considered. Using the BCS solution to the pairing problem the quasiparticle energies E_j are expressed in terms of the relative shell-model orbital energies ϵ_j, the chemical potential λ, and the energy-gap parameter Δ.

The first 28 protons which occupy shell-model orbits up to and including the $1f_{7/2}$ proton orbit and the first 50 neutrons which occupy the $1g_{9/2}$ neutron orbit and below are considered as part of an inert core in the present problem. The protons and neutrons in the "nuclear cloud" outside the core occupy the shell-model orbitals listed in Table IV. Two sets of ϵ_j have been used: those suggested by Kisslinger and Sorensen[9] and a second set chosen to give a smaller occupation of the $3s_{1/2}$ neutron orbit (see Sec. IVC). The chemical potential λ and the gap parameter Δ have been calculated for the proton (neutron) orbits using the pairing constant[9] $G=(26/A)$ $(23/A)$ MeV and the condition that the expectation value of the number operator should give the number of protons (neutrons) in the nucleon cloud.

TABLE IV. The revised set of parameters used in the calculation of the wave functions of Cd^{111}. The strength of the pairing interaction G has been taken from Ref. 9. The chemical potential λ and the gap parameter Δ have been determined from G and the condition: $\sum_j a_j^\dagger a_j$ = the number of nucleons outside the closed shell. The quadrupole phonon energy $\hbar\omega$ is assumed to be the energy of the first excited state in Cd^{110} and is used to determine the interaction strength $\chi_{\lambda=2}$.

	Neutron			Proton		
Δ (MeV)	1.250			0.621		
λ (MeV)	1.685			3.060		
G (MeV)	0.208			0.234		
$\hbar\omega$ (MeV)	0.650					
Orbital	ϵ_j (MeV)	E_j (MeV)	V_j^2	Orbital	ϵ_j (MeV)	E_j (MeV)	V_j^2
$2d_{5/2}$	0.160	1.972	0.88	$1f_{5/2}$	−0.088	3.209	0.99
$1g_{7/2}$	1.400	1.282	0.61	$2p_{3/2}$	0.586	2.551	0.99
$3s_{1/2}$	2.294	1.391	0.28	$2p_{1/2}$	1.628	1.561	0.96
$1h_{11/2}$	2.770	1.655	0.18	$1g_{9/2}$	2.543	0.808	0.82
$2d_{3/2}$	4.600	3.172	0.04				

Ideally, a proper choice of the coupling parameter χ_2 with a simple A dependence would predict the excitation energy $\hbar\omega$ of the first 2^+ state in even-even nuclei. However, because of the great sensitivity of $\hbar\omega$ to χ_2 and in order to include the renormalization of χ_2 resulting from our consideration of only the proton and the neutron clouds, we solve numerically [Eq. (2.27) of Ref. 8] for the value of χ_2 consistent with the experimentally observed energy of the first 2^+ state in Cd^{112}.

Values of the Kisslinger-Sorenson (KS) parameters used in the calculations are listed in Ref. 9. The revised set of parameters is listed in Table IV.

B. Test of the Cd^{111} RPA Wave Function

The spectroscopy of Cd^{111} has been studied by many authors.[20] The level energies, spins, and parities are known for states up to ~1 MeV, and the recent (d,p) and (d,t) stripping measurements of Rosner[22] have established the neutron spectroscopic factors of these levels. It becomes possible then to make quantitative comparisons of the predictions of the RPA calculations with a variety of measurements and thus to obtain some feeling for the relevance of the wave function given in Eq. (5) to the ground state of Cd^{111}.

The eigenvalues and eigenfunctions obtained for Cd^{111} from a complete diagonalization of the Hamiltonian for one choice of unperturbed shell-model energies, ϵ_j, have been reported previously.[9] Because these calculations appear to overestimate the occupation probability of the $3s_{1/2}$ orbit, $V_{1/2}^2$ (see below), a second set of ϵ_j were chosen as mentioned in the previous section. The eigenvalues and eigenfunctions for positive-parity states were obtained with a base which has the phases of Yoshida[8] and includes up to two phonons. They are listed (except for the small two-phonon admixtures) in Table V together with the observed level energies, and

[22] B. Rosner, Phys. Rev. 136, B664 (1964).

TABLE V. The energy levels and wave functions for Cd^{111} resulting from a diagonalization of the Hamiltonian. The coefficients C_{jNIJ} are defined by Eq. (5), where the base vectors $|jNIJ\rangle$ are limited to zero, one, and two phonons. (The two-phonon components are not listed.) The actual eigenvalues can be obtained by adding 0.827 MeV to the differences ΔE_{calc} in column 2.

			C_{j00j}	C_{j12J}			
J	ΔE_{calc} (MeV)	E_{exp} (MeV)	$j=J$	$\frac{1}{2}$	$\frac{3}{2}$	$\frac{5}{2}$	$\frac{7}{2}$
$\frac{1}{2}$	0	0	0.836	···	0.391	−0.256	···
	1.094	1.02	−0.239	···	−0.143	−0.756	···
	1.381	1.19	−0.409	···	0.354	0.031	···
$\frac{3}{2}$	0.293	0.34	0.449	−0.645	0.240	−0.072	0.455
	0.998	0.86	0.012	0.475	−0.105	−0.038	0.784
	1.103	1.55	−0.149	−0.382	−0.493	−0.119	−0.021
$\frac{5}{2}$	0.301	0.245	0.653	−0.372	0.033	−0.531	−0.223
	0.734	0.61	−0.208	−0.814	−0.149	0.263	0.144
	1.023	1.13	−0.163	−0.086	0.143	0.247	−0.880
$\frac{7}{2}$	0.260	0.42	0.901	···	0.213	0.154	−0.286
	0.930	0.70	0.055	···	0.272	0.306	0.747
	1.035		−0.211	···	−0.141	0.715	−0.288

spins.[22] Up to 1 MeV each spin state has appeared twice and there appears to be a one-to-one correspondence. The energy fit is comparable to that of KS with 100–200-keV discrepancies occurring.

A check on the total strength observed for each single-particle orbit in Rosner's work can be achieved by evaluating the sum rule derived by Yoshida [Eq. (5.14a) in Ref. 8]:

$$\text{number of neutron holes in the } j \text{ orbit of the target} = (2j+1) \sum_{\text{observed states}} S_{lj}(d,p)$$

$$= (2j+1)\left[U_j^2 + \left(\frac{2\lambda+1}{2j+1}\right)\sum_{j'} (T_{jj'}{}^{\lambda})^2 V_j^2\right]. \quad (6)$$

A comparison of Rosner's results for $Cd^{110}(d,p)Cd^{111*}$ with the value of the right-hand side of Eq. (6) is shown in Table VI for the two choices of ϵ_j values. In evaluating the sum rule the second term which arises from the quadrupole force is about 60% of the first term for the $2d_{5/2}$ orbit and about 20% for the $3s_{1/2}$ and $1g_{1/2}$ orbits. From Table VI, half of the $1g_{7/2}$ strength has not been observed; but the small (d,p) cross section and the

TABLE VI. The sum-rule prediction of Eq. (6) using the Cd^{111} wave functions of KS (column 2) and of Table V (column 3) are compared to the sums of observed spectroscopic strengths (column 4) for the relevant single-particle orbitals. The values of (column 4) equal $(2j+1)(1-V_j^2)$, where V_j^2 for Cd^{110} is given in Table IV of Ref. 22.

j	KS parameters	Table IV parameters	Observed strengths $\sum(2j+1)S_{lj}$
$\frac{1}{2}$	1.23	1.55	1.8
$\frac{3}{2}$	3.59	3.85	3.2
$\frac{5}{2}$	1.35	1.16	1.5
$\frac{7}{2}$	4.13	3.73	2.0

relatively flat angular distribution expected for such states render them difficult to distinguish. For the other orbits the agreement with both calculations is within about 20% except for the KS comparison with the $3s_{1/2}$ orbit. Here the measured value is 50% larger than the calculations.

A detailed test of the RPA wave functions can be made by comparing the calculated distribution of the spectroscopic strength with the $Cd^{110}(d,p)Cd^{111}$ measurements of Rosner.[22] Using the wave function (4) for $\Psi_{J_iM_i}$ and (5) for $\Psi_{J_fM_f}$, the spectroscopic factor, Eq. (2), for stripping on an even target can be expressed as

$$S_{lj}=\Big[U_jC_{j_f=j,N_i=N_f,v_i=v_f,J_i=I_f,J_f}+[2\lambda+1]^{1/2}V_j\sum_{\substack{j_f,v_f\\N_f,I_f}}(-1)^{J_f+\lambda-J_i-j}C_{j_fN_fv_fI_fJ_f}\begin{Bmatrix}j_f & I_f & J_f\\ J_i & j & \lambda\end{Bmatrix}$$
$$\times\{[N_i(2J_i+1)]^{1/2}(\lambda^{N_f}(I_f)\rangle\!\rangle\lambda^{N_i}J_i)\delta_{N_f,N_i-1}R_{jf_j}^{\lambda}+[N_f(2I_f+1)]^{1/2}(\lambda^{N_i}(J_i)\rangle\!\rangle\lambda^{N_f}I_f)\delta_{N_f,N_i+1}T_{jf_j}^{\lambda}\}\Big]^2, \quad (7)$$

where the first expression in curly brackets is the usual 6_j symbol.

This has been evaluated for the case of $Cd^{110}(d,p)Cd^{111}$ using the positive-parity wave functions of Table V. Figure 15 compares the distribution of the calculated spectroscopic factors (for positive-parity states) with values obtained from the Rosner measurement. The latter are not given in Ref. 22 but were estimated for each state from the formula

$$S_{lj}\,|_{\text{estimated}}=\frac{\dfrac{d\sigma}{d\Omega}(d,p)}{\displaystyle\sum_{\substack{\text{all observed}\\ l,j\text{ states}}}\frac{d\sigma}{d\Omega}(d,p)}\sum_{\substack{\text{all observed}\\ l,j\text{ states}}}S_{lj}, \quad (8)$$

using the data of Tables I and IV of Rosner's paper. This estimate neglects the relatively small Q value dependence of Rosner's DWBA calculation, viz., a 15% increase in the calculated (d,p) cross section per MeV of excitation.[23]

The spectroscopic factors of the lowest $\frac{1}{2}^+$ and $\frac{5}{2}^+$ states in Fig. 15 are in qualitative agreement with experiment while the calculated $\frac{3}{2}^+$ state is a factor of 2 too small. For higher states of these spins the calculated results are consistently small. In a similar comparison using the KS wave functions the calculated value for the lowest $\frac{1}{2}^+$ state is a factor of 2 too small whereas the lowest $\frac{3}{2}^+$ and $\frac{5}{2}^+$ states are in qualitative agreement. In both calculations the concentration of g strength in the lowest $\frac{7}{2}^+$ state is overestimated by a factor of 4. The over-all agreement with the measured spectroscopic factors is qualitatively the same for both calculations. With regard to the ground-state wave function, that listed in Table V gives better agreement with experiment. We proceed therefore to the problem of stripping to phonon states.

C. Spectroscopic Factors for Cd^{112}

Using the wave functions (5) for $\Psi_{J_iM_i}$ and (4) for $\Psi_{J_fM_f}$, the spectroscopic factor Eq. (2) has been calculated for the general case of N phonons in the final state.

$$S_{lj}=\frac{2J_i+1}{2J_f+1}\Big[V_jC_{j_i=j,N_i=N_f,v_i=v_f,I=J_f,J_i}+[2\lambda+1]^{1/2}U_j\sum_{\substack{j_i,v_f\\N_i,I}}(-1)^{J_f-j_i-J_i}C_{j_iN_iv_fIJ_i}\begin{Bmatrix}j_i & I & J_i\\ J_f & j & \lambda\end{Bmatrix}$$
$$\times\{[N_f(2J_f+1)]^{1/2}(\lambda^{N_i}(I)\rangle\!\rangle\lambda^{N_f}J_f)\delta_{N_i,N_f-1}R_{jj_i}^{\lambda}+[(N_f+1)(2I+1)]^{1/2}(\lambda^{N_f}(J_f)\rangle\!\rangle\lambda^{N_i}I)\delta_{N_f,N_i-1}T_{jj_i}^{\lambda}\}\Big]^2, \quad (9)$$

where additional terms involving products of the amplitudes $T_{j_1j_2}^{\lambda}$ and $R_{j_1j_2}^{\lambda}$ have been neglected. In this approximation S_{lj} depends on the sum of two terms which have the selection rules $\Delta N=0$ and $\Delta N=1$, respectively.

The expression (9) has been evaluated using both the ground-state wave function for Cd^{111} of KS and that given in Table V (including the two-phonon admixture not listed) for the cases of zero, one, and two phonons in the final state. In Table VII the calculated results are compared with the measured values.

It would appear that the new choice of parameters gives results for the zero- and one-phonon states in good agreement with experiment. However in comparing the calculated spectroscopic factors for Cd^{112} it is important to understand how the choice of $\epsilon_{1/2}$ affects the result. The experimental sum-rule data (Table IV of Ref. 22) indicates that $V_{1/2}{}^2=0.1$ in Cd^{110} (and 0.2 in Cd^{112}) compared with the calculated value of 0.5 (KS) and 0.3 (present work). A second experimental estimate of this quantity can be obtained by considering the ratio of the two $l_n=0$ spectroscopic factors:

$$\frac{S_{0,1/2}[Cd^{110}(d,p)Cd^{111}(0)]}{S_{0,1/2}[Cd^{111}(d,p)Cd^{112}(0)]}\approx\frac{U_{1/2}{}^2}{2V_{1/2}{}^2},$$

[23] B. Rosner (private communication).

TABLE VII. Comparison of spectroscopic factors. The magnitude of S_{lj} for the zero-, one-, and two-phonon states of Cd^{112} is determined from Eq. (9). The contributions for each neutron orbital and for each term in Eq. (9) are listed separately. Here $S_{lj}=[2/(2J_f+1)](\Delta N=0 \text{ term}+\Delta N=1 \text{ term})^2$. The experimental results (column 7) are compared with results using KS parameters (column 9) and the present work (column 8).

N_f	J_f	Neutron orbital	$\Delta N=0$ term	$\Delta N=\pm1$ term	S_{lj}(calc.)	S_{lj}(exp.)	S_{lj}(calc.)/S_{lj}(exp.)	S_{lj}(KS)
0	0	$3s_{1/2}$	0.443	−0.028	0.344	0.28	1.2	0.649
1	2	$2d_{3/2}$	0.079	0.276	0.050	0.072	0.7	0.136
		$2d_{5/2}$	−0.241	0.191	0.001			0.013
2	0	$3s_{1/2}$	0.085	−0.031	0.006	0.051	0.12	0.016
2	2	$2d_{3/2}$	0.022	0.008	0.0004	≤0.015	≥0.29	0.002
		$2d_{5/2}$	0.110	−0.010	0.004			0.006
2	4	$1g_{7/2}$	0.138	0.085	0.011	≤0.003	>3.7	0.010

where we have used Eqs. (7) and (9) and the fact that for these nuclei the quadrupole-interaction terms for the $j=\frac{1}{2}$ orbits contributes only about 10% to the ratio. Also we assume that $V_{1/2}{}^2$ is essentially the same in Cd^{110} and Cd^{112}. Introducing these experimentally determined spectroscopic factors gives $V_{1/2}{}^2=0.2$. The new set of parameters was in fact chosen to approximate this result. This reduction in the value of $V_{1/2}{}^2$ also brings S_j for the $2_1{}^+$ state into agreement with experiment. This is especially interesting since the largest contribution to this transition (see Table VII) comes from the $\Delta N=\pm1$ term of $S_{l=2,j=3/2}$ and thus depends on the detailed structure of the RPA phonon-creation operator $Q^\dagger$.

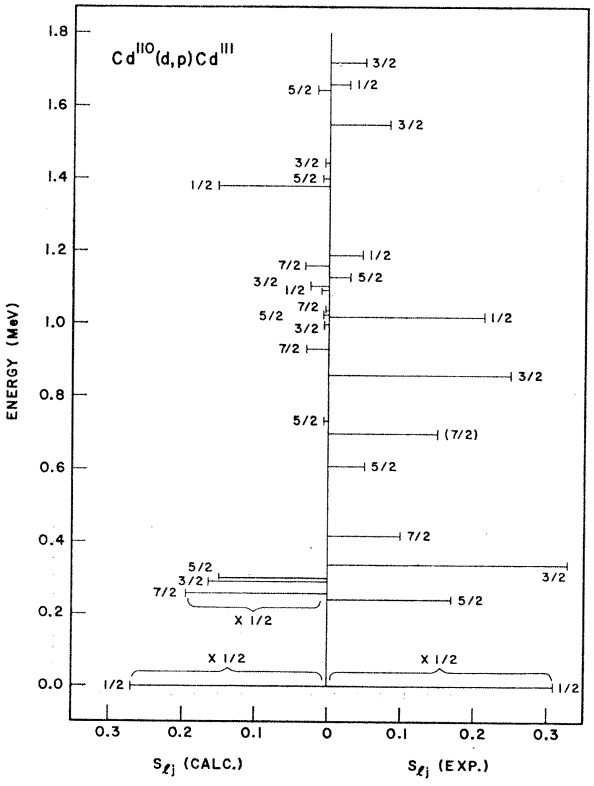

FIG. 15. The observed strength function for the positive-parity states of Cd^{111}, compared to the strength function calculated using the wave functions of Table V.

Comparison between experimental spectroscopic factors for the zero- and one-phonon states and values calculated using the microscopic theory of vibrations have been presented by Sorenson *et al.*[24] using KS wave functions and somewhat different approximations. They find over-all agreement for the ground-state transitions to within 20% and for excited states to within a factor of two for nuclei with $54<A<150$. For Cd^{112} they have predicted $S_{lj}=0.79$ and 0.11; these differ from the results in column 9 of Table VII. For the ground state, the difference arises from their neglect of the $\Delta N=-1$ term; for the one-phonon state, they have neglected the contribution of the two-phonon admixture in the ground state of Cd^{111}.

For the two-phonon states, the situation is less favorable. The calculation predicts an intensity for the $2_2{}^+$ state which is below the sensitivity of the experiment. For the $0_2{}^+$ and $4_1{}^+$ states, the calculations and the experimental results diagree. That the transition strength to the $4_1{}^+$ state is not in agreement is consistent with the poor results for $l_n=4$ transitions for in Cd^{111} (Sec. IV.B). The strong transition to the $0_2{}^+$ two-phonon state is the most direct conflict with the RPA calculations.

The success of the calculations for the zero- and one-phonon states might be taken to imply that the disagreement for the two-phonon states should be assigned to the final-state wave function rather than to the target wave function. However, in evaluating S_{lj}, possible three-phonon admixtures to the target wave function were neglected. For the cases of $N_f=0$ and $N_f=1$, the inclusion of three-phonon admixture in $\Psi_{J_iM_i}$ would have little effect unless terms in products of the amplitudes $R_{jj_i}{}^\lambda$ and $T_{jj_i}{}^\lambda$, neglected in Eq. (9), were also considered. However, for the $N_f=2$ case, a three-phonon component would contribute through the $\Delta N=1$ term in Eq. (9). Considering the small magnitudes of this term for $N_f=2$ in Table VII and noting the significant influence of the small two-phonon admixtures (through the $\Delta N=0$ terms), even a small three-phonon component in $\Psi_{J_iM_i}$ might be important. Finally, the $J_J=0$ and $J_f=2$ levels of the two-phonon

[24] R. A. Sorenson, E. K. Lin, and B. L. Cohen, Phys. Rev. 142, 729 (1966).

state may be admixed with nearby 0^+ and 2^+ levels. Indeed, the 0^+ level at 1.44 MeV and the 2^+ level at 1.47 MeV have strengths comparable to the 0_2^+ and 2_2^+ levels. It is noted (Table IV) that the energies of the lowest pure two-quasiparticle proton states are of this magnitude.

ACKNOWLEDGMENTS

The authors wish to record their sincere appreciation to W. W. Buechner and H. A. Enge of the Massachusetts Institute of Technology and to L. Bollinger of the Argonne National Laboratory for making the experimental facilities available. Particular thanks are due to A. Sperduto and J. Erskine for their help in using the magnetic spectrographs. K. Wetzel helped in taking data and the photographic plates were expertly scanned by Virginia Camp, Masako Nagatani, and Shikuko Miyawaki. Discussions with R. Sorenson, B. Mottleson, and J. Weneser were very helpful in elucidating the theoretical aspects.

PHYSICAL REVIEW VOLUME 155, NUMBER 4 20 MARCH 1967

Spin Determinations of Neutron Resonances in Sb, Ta, Re, and Ir, Using Iron-Alloy Targets

A. STOLOVY
U. S. Naval Research Laboratory, Washington, D. C.
(Received 12 September 1966)

The spin assignments of 14 low-energy neutron resonances in Sb, Ta, Re, and Ir have been made by observing the transmission of polarized neutrons through polarized targets. The nuclei of diamagnetic atoms were polarized by dissolving them in iron, placing the alloy in a magnetic field, and reducing the temperature below 0.1°K. No correlation was found between the resonance spin states and the total radiation widths. Information has also been obtained on the magnitude and direction of the hyperfine fields at the solute nuclei.

INTRODUCTION

SEVERAL years ago, Samoilov and co-workers[1] discovered that large hyperfine magnetic fields could be induced at the nuclei of diamagnetic atoms by dissolving them in iron. The hyperfine field is often of the order of several hundred kOe. By applying a moderate magnetic field to the solid solution and reducing the temperature below 0.1°K, a large nuclear polarization is attainable. We have used this technique to produce polarized targets of several nuclei which would otherwise be very difficult to polarize. The transmission of polarized monochromatic neutrons through these samples was observed in order to determine the spin assignments of 14 resonances. The apparatus and method of taking data have been previously described.[2] Filters were used to reduce the second-order contaminant of the diffracted neutron beam. In most cases, we have supplemented these data with "brute-force" polarization measurements on the pure metals at the larger resonances. The direction and magnitude of the hyperfine fields at the solute nuclei were also obtained, but because of possible inhomogeneities in the alloys, the magnitudes which were obtained must be considered to be lower limits. We have attempted in each case to form a solid solution, using the solubility data given by Hansen.[3]

EXPERIMENTAL RESULTS

In Table I, we have listed our experimental data for both iron-alloy and pure-metal samples. The observed effect $\Delta\tau/\bar{\tau}$ is the percent change in the transmitted beam intensity upon reversing the neutron beam polarization direction. This effect is called positive if it is in the direction we would expect for a $J=I+\frac{1}{2}$ resonance in a nucleus with positive magnetic moment, and with the hyperfine field in the same direction as the applied field. Note that much larger effects have been observed

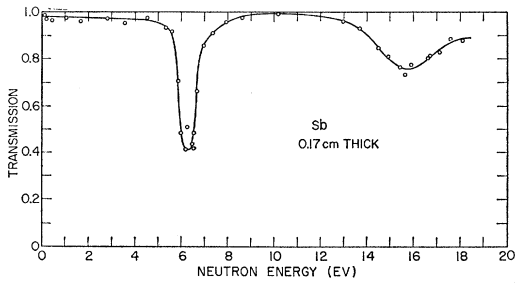

FIG. 1. Transmission plot for Sb metal.

[1] B. N. Samoilov, V. V. Sklyarevskii, and E. P. Stepanov, Zh. Eksperim. i Teor. Fiz. **38**, 359 (1960) [English transl.: Soviet Phys.—JETP **11**, 261 (1960)].
[2] A. Stolovy, Phys. Rev. **118**, 211 (1960).
[3] M. Hansen, *Constitution of Binary Alloys* (McGraw-Hill Book Company, Inc., New York, 1958).